JOURNAL OF MATERIALS SCIENCE 16 (1981) 660–668

Reaction sintering and the α-Si_3N_4/β'-sialon transformation for compositions in the system Si-Al-O-N

M. N. RAHAMAN, F. L. RILEY, R. J. BROOK
Department of Ceramics, The University of Leeds, Leeds, UK

The reaction sintering of three powder compositions corresponding to points near the β'-phase line in the region of $z = 0.75$ has been studied using apparatus which allowed the continuous monitoring of the densification kinetics. The powder compositions were prepared from mixtures of α-Si_3N_4, Al_2O_3 and AlN, and the weight changes in the compacts could be kept to less than $\sim$ 1% over a two hour period. The densification rate is sensitive to small changes in powder composition and decreases markedly as the β'-sialon phase is approached from the oxygen-side. The α-Si_3N_4 to β'-sialon conversion rate, on the other hand, is almost independent of the powder composition. The sintering and transformation kinetic data, combined with surface area measurements and observations on the microstructure of the sintered compacts, indicate that the sintering behaviour is controlled by at least two processes, namely the vapour phase transport of material and a solution–diffusion–reprecipitation process involving a grain boundary liquid phase. Both processes result in the conversion of α-Si_3N_4 to β'-sialon and result in microstructural coarsening but only the second process leads to overall densification in the powder compact.

1. Introduction

Materials based on the system Si–Al–O–N have received considerable attention because of the hope that these materials would be easy to fabricate by pressureless sintering, and that they would have useful high temperature properties [1]. The β'-sialon crystalline phase of theoretical composition $Si_{6-z}Al_zO_zN_{8-z}$, for $0 < z \lesssim 4.2$, has received most attention.

A commonly used starting point for the preparation of such materials is a mixture of α-silicon nitride, aluminium oxide and aluminium nitride. Some detailed studies have already been made of the hot-pressing behaviour of such mixtures with a view to gaining an understanding of the rate controlling mechanisms, and the relationships between composition, densification behaviour and final material properties [2–5].

The decreased driving force for densification during sintering, compared with that available during hot-pressing, means that processes such as evaporation/condensation, surface diffusion and decomposition may become relatively more important. Evaporation/condensation and surface diffusion lead to a gradual smoothing of the grain and pore structure and complicate the task of identifying the rate controlling mechanisms in those sialon compositions which do not contain an appreciable amount of grain boundary liquid phase. Decomposition leading to both weight losses in, and compositional changes of, the powder compact can be minimized by maintaining as near as possible equilibrium partial pressures of gaseous species, such as nitrogen, oxygen and silicon monoxide, over the sample surface. A commonly used method is to surround the sample with a powder bed of silicon nitride containing a small amount of silica, the nitrogen flowing over the powder bed [6–8]. A disadvantage of this method, however, is that sintering measurements can only be made intermittently.

This paper describes an arrangement which

0022–2461/81/030660–09$02.90/0 © *1981 Chapman and Hall Ltd.*

enabled the sintering kinetics of compositions in the system Si–Al–O–N to be monitored continuously. The phase composition, specific surface area and microstructural development at different stages of sintering are reported. Care was taken to keep the weight change of the compact very small. The compositions were prepared from mixtures of α-Si_3N_4, Al_2O_3 and AlN powders. Recent work by Petzow and co-workers [9, 10] has shown that compositions prepared from mixtures of these three powders can be sintered to higher densities, compared with similar compositions prepared from mixtures of α-Si_3N_4, AlN and SiO_2. According to Petzow and co-workers, this is because mixtures containing SiO_2 lead to the formation of a relatively unstable liquid phase which vaporizes during sintering.

The compositions studied in this work corresponded to points near the β'-sialon phase line, with z values in the region of 0.75. A feature of particular interest was the study of the influence of second phases on both the densification and phase transformation kinetics, and of the importance of processes not leading to densification but which might lead to transformation. The sintering kinetics are compared with those for hot-pressing for similar powder compositions at 1963 K and 20 MPa.

2. Experimental procedure

2.1. Materials and preparation.

The powders used were α-Si_3N_4 (~ 90 wt% α, ~ 10 wt% β, median size 6 μm, metallic purity 99.5%) produced by Lucas Industries Ltd, aluminium nitride (99% purity, $< 50\,\mu$m) supplied by Koch-Light Laboratories Ltd, and alumina (Alcoa A-16 superground, median size 1 μm, purity $> 99.9\%$). Scanning electron microscopy (SEM) showed that the α-Si_3N_4 powder contained a small amount of lath-like particles having lengths of up to $\sim 10\,\mu$m. An SiO_2 level of 4 wt% on the Si_3N_4 powder together with an Al_2O_3 level of 6 wt% on the AlN powder were assumed on the basis of neutron activation analysis performed elsewhere [11].

Table I shows the three sample compositions studied (code letters A, C and E). The amounts of α-Si_3N_4, AlN and Al_2O_3 are shown in weight per cent. A carefully controlled procedure was used to prepare the powder mixtures. 10 g of powder and 25 cm^3 of propan-2-ol were milled in a vibro-mill for 30 min using a polyethylene container and alumina grinding pellets. After milling, the powder was dried and formed into 1 g cylindrical pellets by die-pressing followed by isostatic pressing at 200 MPa. The phase compositions (in equivalent %) of A, C and E were calculated taking into account the oxide contents of Si_3N_4 and AlN and the amount of Al_2O_3 gained during milling.

TABLE I The powder composition of materials A, C and E

Sample	Powder composition (wt%)			Phase composition (equivalent %)	
	Si_3N_4	Al_2O_3	AlN	Al	O
A	90.3	3.7	6.0	8.5	6.4
C	87.4	9.0	3.6	10.3	10.1
E	84.6	14.0	1.4	12.0	13.6

2.2. Apparatus

The sintering apparatus is shown schematically in Fig. 1. The powder pellet, surrounded by a loosely fitting silicon nitride cylinder, was placed inside a fully dense, hot-pressed sialon crucible. The silicon nitride used for making the cylinder was identical to that used for preparing the pellet and served to maintain as near as possible equilibrium partial

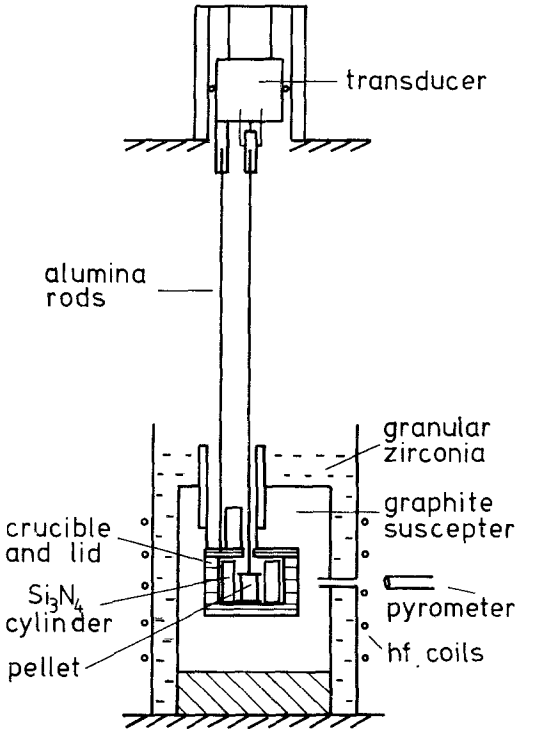

Figure 1 Schematic diagram of the high temperature sintering apparatus.

pressures of gaseous species over the sample surface. Continuous measurement of sintering shrinkage was made using two high-purity alumina push-rods and a sensitive transducer (Philips PR9310), the output of which was fed to a chart recorder. One push-rod, connected to the transducer body, rested on the crucible lid. The other, connected to the moveable armature, passed through a hole drilled centrally in the crucible lid and rested on a sialon spacer placed on the pellet. The transducer and push-rods were counterbalanced in order to minimize the load on the pellet. Sintering temperature (in most experiments 1963 K) could be obtained in 15 min, the last 200 K being covered in 2 min.

2.3. Measurements and microstructural examination

Initial experiments were performed to determine the sinterability, phase and weight changes of the powder compositions at different temperatures. In these experiments, compositions A and E were sintered for 1 h at four temperatures between 1823 and 2033 K.

In a series of more detailed experiments, compositions A, C and E were sintered at 1963 K for 2 h with the shrinkage (ΔL) being measured continuously. Measurements of the final lengths of the pellets were obtained subsequently, and used to provide a measurement of the initial length, (L_0). The final densities of the pellets were measured using a mercury-upthrust method [12]. The density at a given time was calculated from the final density and the value for (ΔL) at that time. A theoretical density of 3150 kg m^{-3} was assumed for β'-sialon in the compositional region studied.

In a separate series of experiments at 1963 K, sintering was terminated by rapid cooling after a series of times ranging from 0 to 120 min. "Zero" time corresponded to heating to sintering temperature followed by immediate cooling. These pellets were then crushed and analysed for α-Si_3N_4 and β'-sialon contents using filtered CuKα radiation. The amounts of α-Si_3N_4 remaining and β'-sialon formed were determined from the peak heights of the α_{201}, β'_{101} and β'_{210} reflections using MgO as an internal standard. The α-Si_3N_4 and β'-sialon contents could be assessed to better than ± 3%.

The specific surface area of sintered compacts was measured by the single point BET method using a continuous flow of 30% N_2 in He. The microstructure of typical etched (40% HF + 100% HNO_3, 1:1 by volume, 298 K, 5 min) fracture surfaces was examined using a Cambridge S600 scanning electron microscope.

3. Results

3.1. The effect of temperature on the densification and conversion behaviour

Fig. 2 compares the relative density, ρ, and the weight change, ΔW, in the powder compact for compositions A and E after sintering for 1 h at four temperatures between 1823 and 2023 K. A positive value for ΔW denotes a weight gain in the powder compact. ΔW is very small; for composition A there is a weight gain but composition E loses weight above ~ 1898 K. It can be seen that composition A undergoes only a small amount of densification even at temperatures up to 2023 K. The density of composition E, however, increases more rapidly above ~ 1923 K. The specific surface areas (Table II) differ only slightly, even above ~ 1923 K when composition E has densified very much more than composition A. Scanning electron micrographs of fracture surfaces of composition E sintered for 1 h at 1823 and 2023 K are shown in Fig. 3. The micrograph at 1823 K appears similar to that of a green compact; the one at 2023 K,

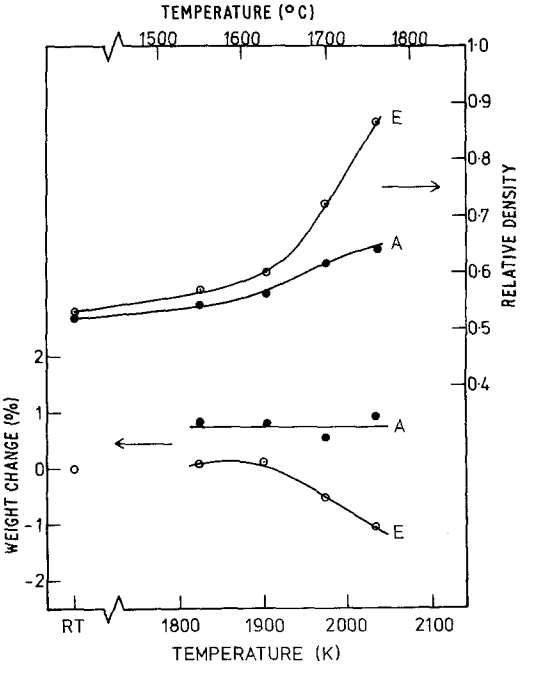

Figure 2 Relative density and weight change for compositions A and E after 1 h at different temperatures.

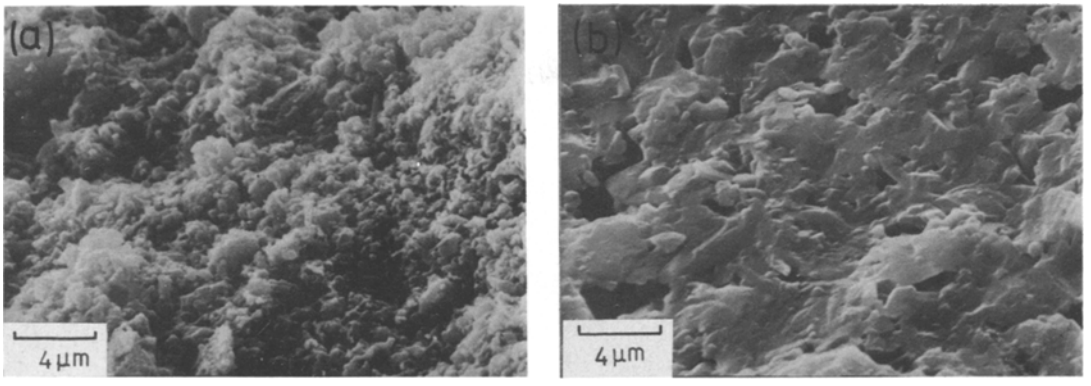

Figure 3 Scanning electron micrographs of etched fracture surfaces of composition E after 1 h at (a) 1823 K and (b) 2033 K.

however, shows a significant amount of particle–particle bonding and grain growth.

The α-Si_3N_4 and β'-sialon phase contents are shown in Fig. 4. It can be seen that in contrast to the densification behaviour, the phase contents of compositions A and E after a series of identical sintering treatments, differ only slightly. It should also be noted that at 1898 K there is considerable conversion (~ 60% β'-sialon formed) although the density has increased by only ~ 8% for composition A and ~ 12% for composition E.

3.2. The effect of time on the densification and conversion behaviour

The effect of sintering time, t, on the fractional shrinkage $(\Delta L/L_0)$, and the relative density, ρ, for compositions A, C and E at 1963 K is shown in Fig. 5. The curves shown are the smoothed average curves obtained from four separate runs for each composition. At any time, both $(\Delta L/L_0)$ and ρ increase as the composition changes from A and E.

Fig. 6 shows the changes in phase composition occurring with time for compositions A and E at 1963 K. The results for composition C are situated between those for A and E. The differences in phase content at any time are small for these compositions. Over an appreciable time range, between about 5 and 75 min, the decrease in α-Si_3N_4 content can be described by a first order rate law.

TABLE II Specific surface areas of green compacts and compacts sintered for 1 h at different temperatures

Composition	Specific surface area ($m^2\ g^{-1}$)				
	Green	1828 K	1898 K	1963 K	2033 K
A	6.2	4.2	3.7	3.0	2.5
E	6.6	4.5	4.2	2.9	2.0

Fig. 7 shows the scanning electron micrographs of a green pellet and of typical etched fracture surfaces of pellets of composition A after sintering for 1 and 2 h respectively. It is seen that considerable microstructural changes have occurred even though the relative density has only increased from a green value of ~ 0.53 to ~ 0.63 after 2 h.

4. Discussion

It is clear from Fig. 5 that the sintering behaviour of these compositions is sensitive to small departures in composition from those corresponding to the β'-sialon line. In this respect sintering behaviour at 1 atm external pressure shows features identical to those observed during hot-pressing. For comparison, relative densification rates at a constant relative density of 0.625 are plotted as a function

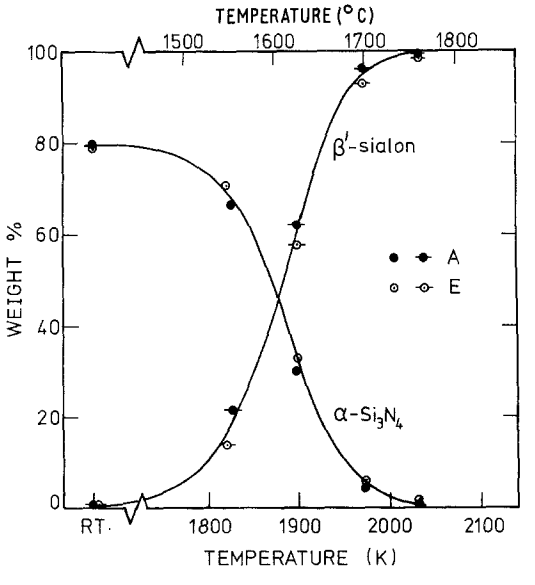

Figure 4 α-Si_3N_4 and β'-sialon contents for compositions A and E after 1 h at different temperatures.

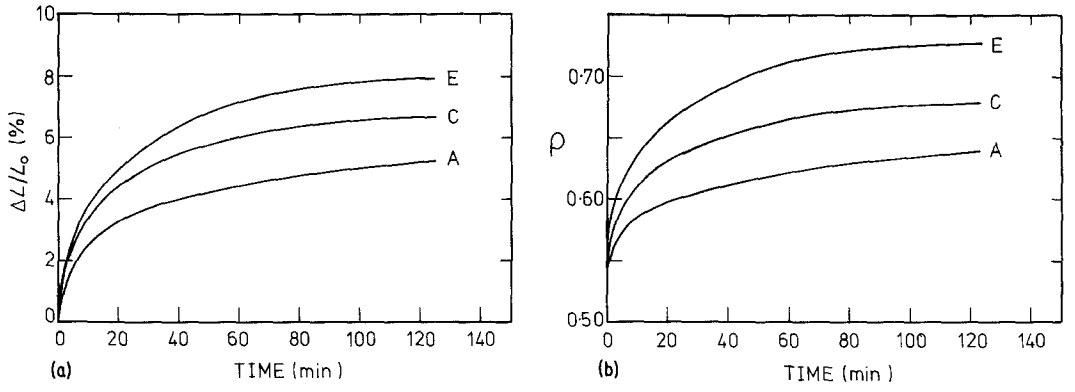

Figure 5 Smoothed average curves of (a) fractional shrinkage and (b) relative density against time for compositions A, C and E at 1963 K.

of the second phase content of each composition in Fig. 8. The second phase content is obtained from the tie line passing through each composition and connecting the β'-phase line with the liquid phase region on the isothermal Si–Al–O–N behaviour diagram. The tie lines and behaviour diagram used are those given by Naik *et al.* [13]. It is seen that the densification rate decreases with decreasing second phase content for composition E to composition A. These densification rates are approximately two orders of magnitude slower than those observed for the same compositions during hot-pressing at 1963 K under 20 MPa pressure [5].

It can be seen that the sintering rate becomes very small as the powder composition approaches that of β'-sialon from the SiO_2 side. This data is fully consistent with the view that the presence of a liquid phase is necessary for densification and indicates that a process of solution–diffusion–reprecipitation is of considerable importance under these conditions. Moreover the results of Fig. 2 indicate that the sintering temperature must be above ~ 1923 K for appreciable densification to take place in composition E.

Analysis of the results of Fig. 5 in terms of the Kingery liquid phase sintering models [14] proved unhelpful. Plots of $\log(\Delta L/L_0)$ against $\log t$ for the results of Fig. 5 gave slopes which continuously decreased with time. In these models, after an initial particle rearrangement stage, uniform slopes of 1/3 or 1/5 would be expected depending on the exact geometries and rate controlling processes assumed. The limited application of such models

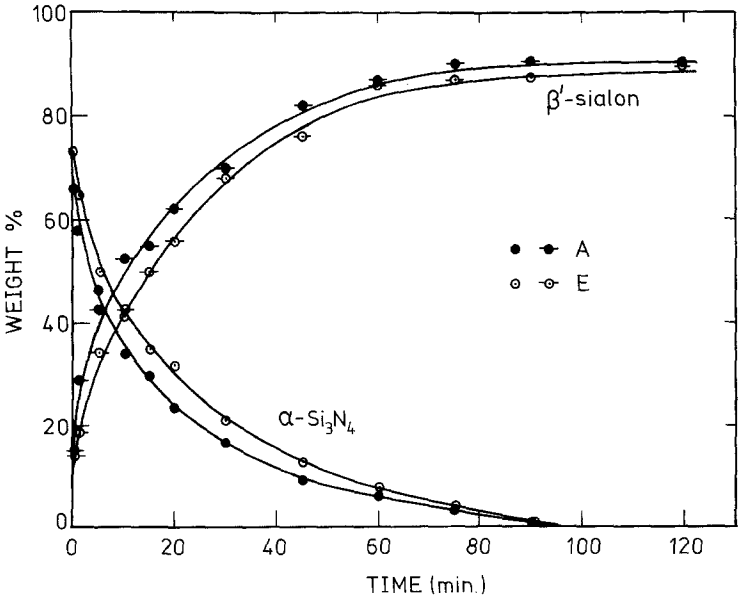

Figure 6 α-Si_3N_4 and β'-sialon contents against time for compositions A and E at 1963 K.

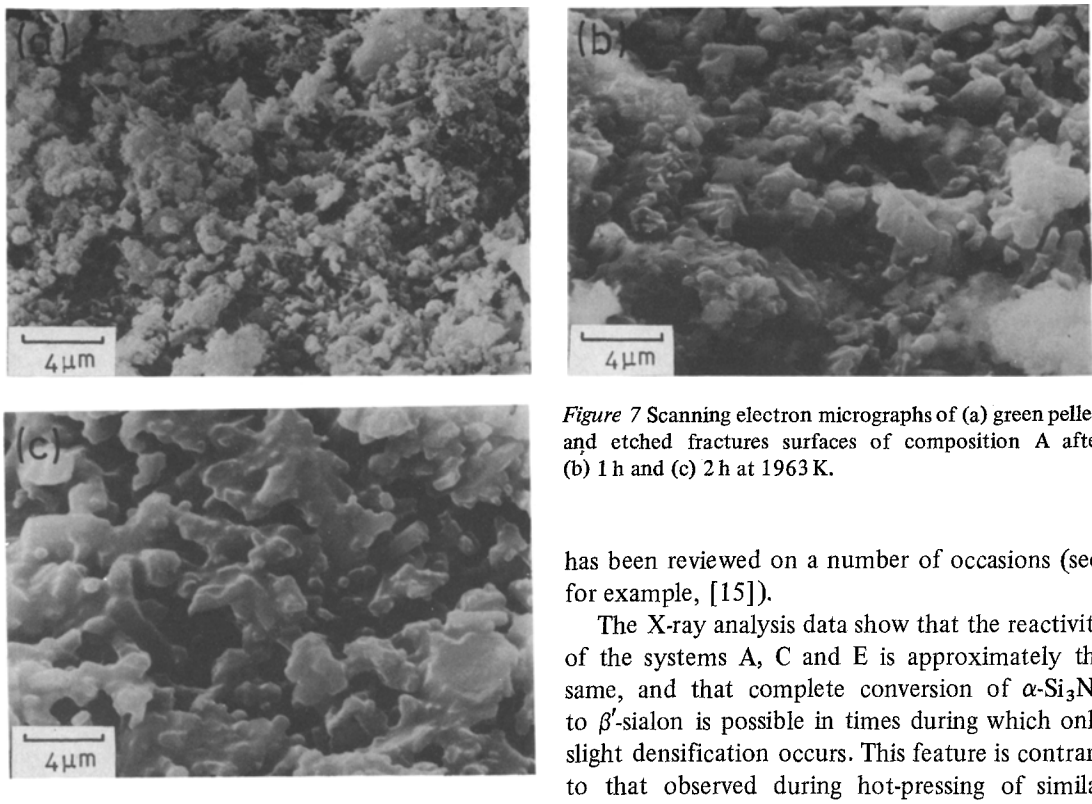

Figure 7 Scanning electron micrographs of (a) green pellet, and etched fractures surfaces of composition A after (b) 1 h and (c) 2 h at 1963 K.

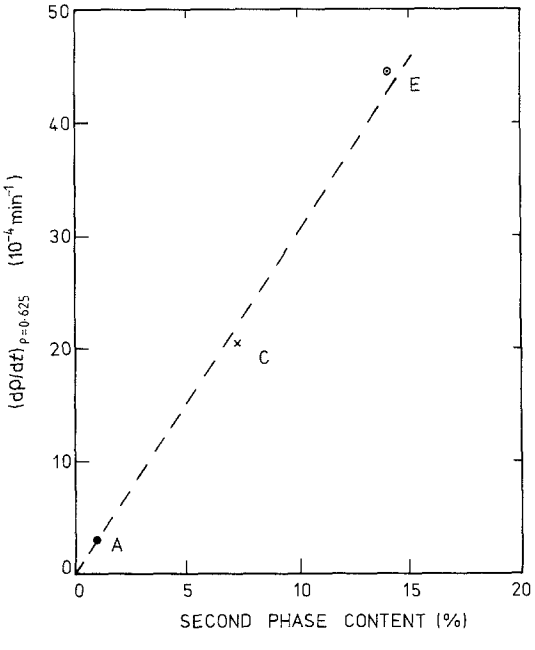

Figure 8 Relative densification rate at a relative density of 0.625 against second phase content for compositions A, C and E at 1963 K.

has been reviewed on a number of occasions (see, for example, [15]).

The X-ray analysis data show that the reactivity of the systems A, C and E is approximately the same, and that complete conversion of α-Si_3N_4 to β'-sialon is possible in times during which only slight densification occurs. This feature is contrary to that observed during hot-pressing of similar systems, and for which at larger liquid phase contents the conversion rate constant shows a distinct dependence on the amount of liquid phase initially expected to be present [16]. At the same time, the microstructural examinations using scanning electron microscopy, shown in Fig. 7, indicate that the β'-sialon has a mean grain size considerably larger than that of the starting α-sialon nitride powder.

All of these features suggest that important non-densifying processes which lead to conversion and microstructural coarsening are available in this system. Two such processes are surface diffusion and evaporation/condensation. For these primarily covalent bonded materials, evaporation/condensation appears to be the more probable process. Silicon nitride has an effective vapour pressure, as given by the dissociation

$$Si_3N_4(s) \rightleftharpoons 3Si(g) + 2N_2(g) \qquad (1)$$

of the order of 10^{-3} atm at $\sim$ 1963 K, if a pressure of nitrogen of 1 atm is assumed [17]. The rapid vapour phase transport of silicon nitride from the α-Si_3N_4 crystallites to the developing β'-sialon nuclei within the liquid phase would provide a mechanism for the α-Si_3N_4 to β'-sialon conversion. At the same time, through the filling of neck

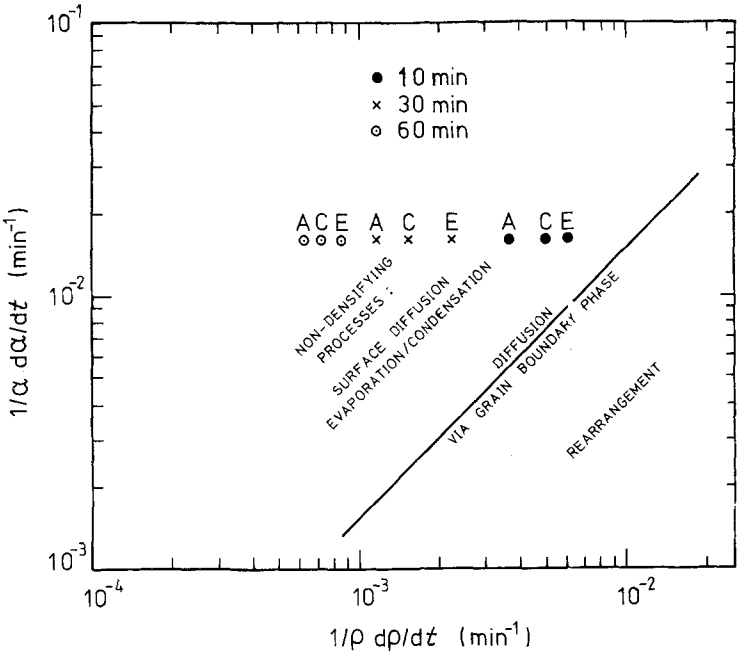

Figure 9 Relation between conversion and densification rates for compositions A, C and E after different times at 1963 K.

regions at crystal contact points, the stress gradients providing the driving force for the grain boundary diffusion of material are reduced. Thus the difficulty in sintering compositions containing relatively little liquid phase can be explained, on the basis of interfering material transport by a process of evaporation and condensation.

Additional evidence in favour of the importance of non-densifying processes which lead to conversion and microstructural coarsening is derived first, from a direct comparison of the densification and conversion rates and secondly, from surface area measurements of the sintered compacts. In Fig. 9 the normalized conversion rate, $(1/\alpha)(d\alpha/dt)$, is plotted against the normalized densification rate, $(1/\rho)(d\rho/dt)$, for compositions A, C and E at different sintering times. For diffusion by way of a second phase at the grain boundary [18, 19], a relation of the form

$$\left(\frac{1}{\alpha}\frac{d\alpha}{dt}\right) = -\frac{3}{2}S\left(\frac{1}{\rho}\frac{d\rho}{dt}\right) \qquad (2)$$

has been derived for the association of the conversion step with the diffusion step [20]. S is the probability that the diffusing atom takes part in the conversion and is taken to be 1 for the solid line shown in Fig. 9. For the compositions studied, the results are in the region of the diagram for which non-densifying processes which lead to conversion are significant. The role of these processes becomes more important at longer times, as seen by the shift of the data points towards the left of the diagram.

The specific surface area, S_s, of compositions A and E (see Table II) is plotted against relative density, ρ, in Fig. 10. De Hoff *et al.* [21] have shown from topological considerations that the trajectory of the S_s against ρ plot during second stage densification is a straight line connecting the initial and final stages. For non-densifying processes which lead to particle coarsening, the trajectory is a straight line parallel to the S_s axis. The trajectory of the S_s against ρ plot lies between these two extremes when both non-densifying and densifying processes occur. It is clear from Fig. 10 that there are significant contributions from non-densifying processes; moreover these processes are relatively more dominant in composition A. It should also be noted that S_s for composition E at $\rho \sim 0.86$, obtained for the compact sintered at 2033 K, lies approximately on the densification trajectory. This is a reasonable result since at this temperature composition E contains an appreciable amount of liquid phase, and the liquid phase densification process is expected to have become dominant. At lower temperatures the amount of liquid phase is less and the non-densifying processes become relatively more dominant with the result that the S_s against ρ data points lean more towards the coarsening trajectory.

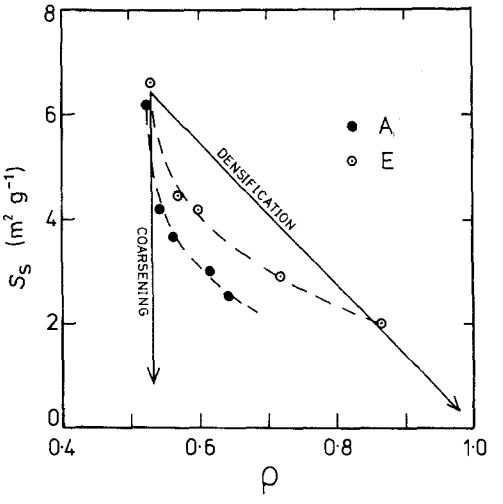

Figure 10 Specific surface area against relative density for sintered compacts of compositions A and E.

For these systems, with at least two major material transport processes operating, it would not be expected that densification data could be fitted to any simple, single rate equation. In this general respect, compositions close to those of β'-sialon show features closely similar to those of the covalent silicon, silicon carbide and silicon nitride, for which special conditions (including the use of suitable liquid phases) are necessary for densification during sintering [22].

5. Conclusions

The results show that, with the sintering arrangement used, it is possible to monitor continuously the densification kinetics during reaction sintering of powder compositions in the system Si–Al–O–N, and also keep the weight losses in the compact small, ~ 1% over a 2 h period at 1963 K.

The densification rate is sensitive to changes in powder composition and decreases markedly as the composition approaches that of β'-sialon. The conversion rate, on the other hand, is almost independent of the composition of the powders studied.

The sintering behaviour is controlled by at least two processes, namely the vapour phase transport of material and a solution–diffusion–reprecipitation process involving a grain boundary liquid phase. Both processes result in the conversion of α-Si_3N_4 to β'-sialon and result in microstructural coarsening, but only the second process leads to overall densification in the powder compact. Moreover, the temperature of the compact must be above ~ 1923 K for the liquid phase process to operate significantly.

A significant volume of grain boundary liquid phase is required before the rate of densification becomes comparable with the rate of the densification-retaining vapour phase transport process. For this reason, powder compositions corresponding exactly to the β'-sialon line and containing initially only very small quantities of liquid phase, cannot be densified to any appreciable extent during sintering with powders of conventional particle size range.

Acknowledgments

The support of this work by the Science Research Council through a Research Grant is acknowledged. The authors wish to thank M. Benn for help in the design of the apparatus and the staff of the Houldsworth School Workshop for technical help in its construction.

References

1. K. H. JACK, *J. Mater. Sci.* **11** (1976) 1135.
2. M. H. LEWIS, B. D. POWELL, P. DREW, R. J. LUMBY, B. NORTH and A. J. TAYLOR, *ibid.* **12** (1977) 61.
3. M. BENN, M. KUWABARA and F. L. RILEY, in "Science of Ceramics", Vol. 9, edited by K. J. de Vries (Ned. Keramische Vereniging, Stoke on Trent, 1977) p. 119.
4. A. W. J. M. RAE, D. P. THOMPSON and K. H. JACK, Proceedings of the Army Materials Technology Conference, "Ceramics for High Performance Applications – II", edited by J. J. Burke, E. M. Lenoe and R. N. Katz (Brook Hill, Massachusetts, 1978) p. 1039.
5. M. N. RAHAMAN, F. L. RILEY and R. J. BROOK, *J. Amer. Ceram. Soc.*
6. L. J. GAUCKLER, S. BOSKOVIC, G. PETZOW and T. Y. TIEN, in "Nitrogen Ceramics", edited by F. L. Riley, NATO ASI, Applied Science Series No. 23 (Noordhoff, Leyden, 1977) p. 405.
7. M. MITOMO, N. KURAMOTO and Y. INOMATA, *J. Mater. Sci.* **14** (1979) 2309.
8. M. BENN and F. L. RILEY, *ibid.* **15** (1980) 529.
9. G. PETZOW, L. J. GAUCKLER, T. Y. YIEN and S. BOSKOVIC, in Proceedings of the International Symposium on Factors in Densification and Sintering of Oxide and Non-Oxide Ceramics, edited by S. Somiya and S. Saito, Hakone (Tokyo Institute of Technology, Japan, 1979) p. 28.
10. S. BOSKOVIC, L. J. GAUCKLER, G. PETZOW and T. Y. TIEN, in "Sintering Processes", edited by G. C. Kuczynski (Plenum Press, London, 1980) p. 295.
11. B. NORTH, M.Sc. Thesis, University of Birmingham, 1978.
12. D. R. ASHWORTH, *J. Brit. Ceram. Soc.* **6** (1979) 70.

13. I. K. NAIK, L. J. GAUCKLER and T. Y. TIEN, *J. Amer. Ceram. Soc.* **61** (1978) 332.
14. W. D. KINGERY, *J. Appl. Phys.* **30** (1959) 301.
15. D. L. JOHNSON, in "Ultrafine Grain Ceramics", edited by J. J. Burke, N. L. Reed and V. Weiss (Syracuse University Press, New York, 1970) p. 173.
16. M. KUWABARA, M. BENN and F. L. RILEY, *J. Mater. Sci.* **15** (1980) 1407.
17. JANAF Thermochemical Tables (2nd edition), US Dept. of Commerce (1971).
18. R. L. COBLE, *J. Appl. Phys.* **34** (1963) 1679.
19. *Idem, ibid.* **41** (1970) 4798.
20. L. J. BOWEN, T. G. CARRUTHERS and R. J. BROOK, *J. Amer. Ceram. Soc.* **61** (1978) 335.
21. R. T. DE HOFF, R. A. RUMMEL, H. P. LA BUFF and F. N. RHINES, in "Modern Developments in Powder Metallurgy", Vol. 1, edited by H. H. Hausner (Plenum Press, New York, 1966) p. 310.
22. C. GRESKOVICH and J. H. ROSOLOWSKI, *J. Amer. Ceram. Soc.* **59** (1976) 336.

Received 28 July and accepted 1 August 1980.